Northumbria Research Link

University**Library**

Vehicular VLC: A Ray Tracing Study Based on Measured Radiation Patterns of Commercial Taillights

Hossien B. Eldeeb[1], Elizabeth Eso[2], Elnaz Alizadeh Jarchlo[3], Stanislav Zvanovec[4], Murat Uysal[1], Zabih Ghassemlooy[2], and Juna Sathian[2]

Abstract—In this paper, we investigate the performance of vehicular visible light communications based on the radiation patterns of different commercial taillights (TLs) using non-sequential ray tracing simulations. Our simulation results indicate a significant variation in the path loss compared with Lambertian model. Based on the ray tracing results, we propose a new path loss model as a function of the propagation distance considering the asymmetrical radiation pattern of TLs. We use this model to derive the attainable transmission distance. We further present the delay spread for various vehicular communication scenarios to demonstrate the effect of neighboring vehicles.

Index Terms— *Visible light communications, asymmetrical radiation pattern, ray tracing, path loss, commercial vehicle taillights*

I. INTRODUCTION

NOWADAYS, there are growing research interests in vehicular communications with the aim of improving driving safety and reducing road fatalities. To this effect, many governments and global organizations have shown interest in the concept of intelligent transportation systems (ITS), which is mostly dominated by the radio frequency (RF) wireless technologies. In recent years, a growing number of research works have demonstrated the feasibility of optical wireless communications technologies in ITS [1,2]. This is helped with the widespread use of light emitting diodes (LEDs)-based headlights (HLs) and taillights (TLs) in vehicles, which facilitates implementation of vehicular visible light communications (VVLC) [1,2]. Channel modeling plays an important role in VLC links as in any other communication techniques since it has a great impact on the link power and bandwidth budgets. In VLC, the link path loss (PL) can be obtained using ray tracing and experimental measurements. Extensive experimental and simulation studies on the VLC link loss are reported in the literature [3-5]. In [3], the main optical channel characteristics that affect the VLC link performance in the VVLC networks were investigated. In [4], the performance

1 Department of Electrical and Electronics Engineering, Ozyegin University, Istanbul, Turkey.
2 Optical Communication Research Group, Faculty of Engineering and Environment, Northumbria University, Newcastle, UK.
3 Department of Telecommunication Systems, Technische Universität Berlin, Berlin, Germany.
4 Department of Electromagnetic Field, Faculty of Electrical Engineering, Czech Technical University, Prague, Czech Republic.

limits of VLC based on HLs were evaluated for vehicle-to-vehicle (V2V) communications. In [5], a measured HL radiation pattern model was adopted, and the relationship between the system bit error rate (BER) performance and the transmission span was investigated.

However, there are only a few studies focused on the use of TLs in VVLC [6-8]. In [6], the radiation pattern of HL and brake light was measured considering only one commercial brand, and a channel PL model was proposed for the HL Tx. In [7], an analytical study of the VLC channel model in a realistic V2V setting was carried out, which estimated the received power P_r of the scooter TL for distances up to 10 m. In [8], the link asymmetry problem of V2V was identified with a significant difference in P_r for incoming and outgoing links. Recently, the radiation pattern of a commercial's TL was measured [9], showing that TL has a non-symmetric pattern, which is different from the Lambertian model.

In this paper, we extend the work in [9] firstly, by using real measured radiation patterns for commercially available TLs from different automotive manufacturers i.e., BMW, Audi A5, and Nissan. Since the measured TL's radiation patterns have an asymmetrical profile, an alternative PL model to commonly used Lambertian model becomes essential. To achieve this, we have utilized the ray tracing approach using OpticStudio® for channel modeling, which was used in the development of IEEE 802.15.13 and 802.11bb reference channel models and validated in [10] through extensive measurements. Specifically, we incorporate the measured radiation pattern of TL using the 3D simulation platform. From non-sequential ray tracing, we obtain the corresponding channel impulse responses (CIRs) and derive a new PL model. Next, we estimate the performance of VVLC in terms of the maximum transmission distance at a target BER. Furthermore, the root-mean-square (RMS) delay spread is investigated by considering different V2V scenarios.

II. CHANNEL MODELING

A. Lambertian Approach

The ideal Lambertian model is widely used to obtain the CIRs of VLC channels. In this approach, any light source is assumed to have a regular radiation pattern with the luminous intensity defined as a function of the irradiance angle α. Let $n_L = -\ln(2)/\ln(\cos(\theta_{1/2}))$ be Lambertian order at the half-power angle $\theta_{1/2}$. For a propagation distance of d and the incidence angle of β, the CIR is given by [3]:

$$h(t) = \frac{(n_L+1)A}{2\pi d^2} \cos^{n_L}(\alpha) \cos(\beta) \delta\left(t - \frac{d}{c}\right), \tag{1}$$

where A is the photodetector (PD) area, and c is the light speed.

B. Ray Tracing Approach

Lambertian model matches well with most indoor light sources, but not with the outdoor lights, i.e., HLs [4], TLs [9], because of asymmetrical radiation patterns designed for different illumination applications. To consider the characteristics of outdoor light sources, a non-sequential ray tracing approach [4,9] can be used where the measured radiation pattern is imported into the 3D simulation platform constructed using OpticStudio. The main steps involved are as follows: (*i*) creating a 3D simulation model of the test environment and importing the embedded CAD models of the objects; (*ii*) defining the coating materials (reflectance and scattering) of CAD; (*iii*) defining the system parameters including the radiation patterns, optical transmit power levels, Txs and Rxs orientations, angular field-of-view (AFOV) of the PD and its active area; and (*iv*) performing non-sequential ray-tracing to obtain the path length and emitted power per ray from the Tx (TL) to the Rx. The collected data is exported into MATLAB® for processing. Finally, the CIR is obtained as [3]:

$$h(t) = \sum_{k=1}^{M} P_k \delta(t - \tau_k), \tag{2}$$

where M is the number of rays received at the PD, and δ is Dirac delta function. P_k and τ_k, respectively denote the power and the propagation delay of the kth ray, and $k = 1, 2, \ldots, M$. The PL is given by:

$$PL = 10\log_{10}\left(\int_0^\infty h(t)dt\right). \tag{3}$$

III. RADIATION PATTERNS OF TLS

Three vehicle TLs from (a) BMW F30 right side outer LED O/S TL (BMW), (b) Audi A5 S5 N/S LED left outer TL facelift (Audi), and (c) Nissan Qashqai tailgate boot lid right side 26550 4EA0A model TL (Nissan) are used in this work. To empirically obtain the TLs optical radiation patterns, we have used an optical power meter (Thorlabs PM100D) to measure P_r over a fixed d of 1 m for -90° $< \theta < +90°$.

The measured radiation patterns of the TLs under investigation are shown in Fig. 1 along with the benchmarking Lambertian pattern. The measured key parameters are listed in Table 1. The half power angle (HPA) of each TL, which is the angle in degrees between the peak and the point on one side of the beam axis (left or right) where P_r is half the maximum, is measured. As shown in Table 1, there is a wide variation in the parameters. For example, BMW and Nissan TLs have wide and narrow HPA values of 75° and 65°, and 27° and 22° to the left and right of their beam axis, respectively.

It is observed from Fig. 1 that TLs have an asymmetrical pattern, which depends on HPA with the pattern direction being shifted (inclined) with respect to the reference direction of 0° and cannot be described by the ideal Lambertian profile. For example, in Nissan TL, see Fig. 1(c), the pattern direction is
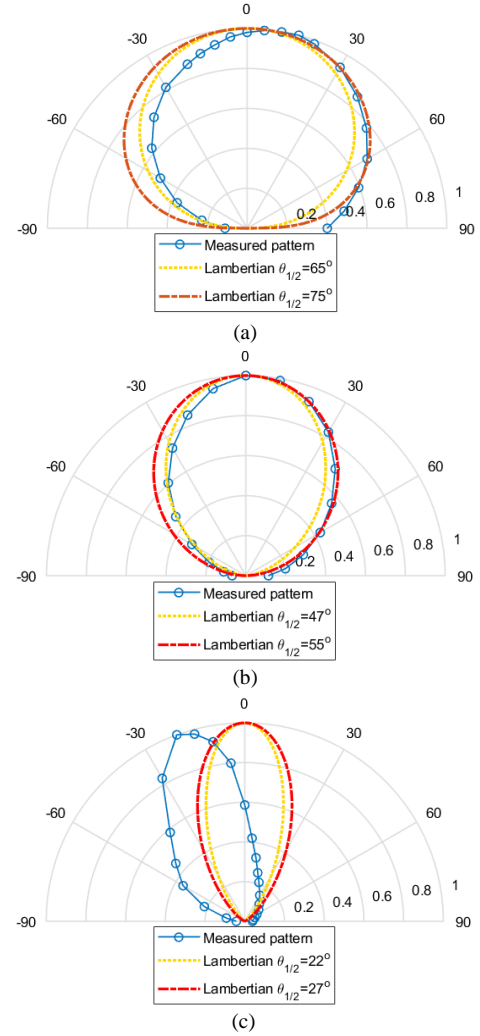

(a)

(b)

(c)

Fig. 1. Measured and Lambertian patterns for: (a) BMW, (b) Audi, and (c) Nissan.

TABLE I
TL PARAMETERS FROM EMPIRICAL MEASUREMENTS

TL brand	θ - left (°)	θ -right(°)	P_t (mW)	ε_i	ζ_i
(a) BMW	65	75	111	0.809	0.074
(b) Audi	47	55	40	0.801	0.072
(c) Nissan	22	27	9	0.805	0.079

significantly shifted by 20° with respect to the 0° direction, which of course will influence the channel path loss.

IV. PATH LOSS MODEL AND PERFORMANCE ANALYSIS

In this section, we use the obtained CIRs using the ray-tracing approach to propose a new expression for the channel PL based on the data fitting. The new PL model is an explicit function of d and the vehicle's TL, which is given by:

$$PL_i(d) = PL_{0,i} + 10\log_{10}\left(d^{-2\varepsilon_i}\right) - \zeta_i d, \ i \in \{a,b,c\} \tag{4}$$

where PL_0 is the reference PL at d_0 of 1 m. The values of ε_i and ζ_i are determined by means of ray tracing simulation for each model as given in Table I.

For the non-return to zero on and off keying (NRZ-OOK) data format, the BER is given by:

$$BER_i(d) = \frac{1}{2}\text{erfc}\left(\frac{\sqrt{\gamma_i(d)}}{2\sqrt{2}}\right), \tag{5}$$

In (5), γ_i is the signal-to-noise-ratio (SNR) and is given by:

$$\gamma_i(d) = \frac{(\eta R H_i(d))^2 P_e}{\sigma_n^2}, \tag{6}$$

where η is the electrical-optical conversion factor, R is PD's responsivity, σ_n^2 is the noise variance, P_e is electrical power at the Tx, and $H_i(d)$ is the channel DC gain at d. Substituting (6) in (5) and solving for $H_i(d)$, we have:

$$H_i(d) = 2\sqrt{2}\left(\sqrt{\frac{\sigma_n^2}{P_e\eta^2 R^2}}\right)\text{erfc}^{-1}\left(2BER\right). \tag{7}$$

$H_i(d)$ can also be obtained from (4) as:

$$H_i(d) = 10^{\left(\frac{PL_{0,i}}{10} + \log_{10}\left(d^{-2\varepsilon_i}\right) - \frac{\zeta_i}{10}d\right)}. \tag{8}$$

Using (8) and (7) and substituting for $\sigma_n^2 = N_0 B_w$, where N_0 is the noise power spectral density, and B_w is the noise bandwidth, the transmission range at the threshold BER (BER$_T$) is expressed as:

$$d_i = \frac{20\log_{10} e}{\zeta_i / \varepsilon_i} W\left[\frac{\zeta_i / \varepsilon_i}{20\log_{10} e}\exp\left(\frac{\frac{PL_{0,i}}{10} - \log_{10}\left(2\sqrt{2}\left(\sqrt{\frac{N_0 B_w}{P_e\eta^2 R^2}}\right)\text{erfc}^{-1}\left(2BER_T\right)\right)}{2\varepsilon_i\log_{10} e}\right)\right] \tag{9}$$

where W denotes Lambert wave function.

V. RESULTS AND DISCUSSION

In this section, we present the simulation results for PL, delay spread, and attainable d for $R = 0.54$, $P_e = 10$ W, $N_0 = 10^{-22}$ W/Hz, B_w corresponds to 100 kHz, 1 MHz, and 5 MHz, and $\eta = 0.5$. We assume an asphalt road surface with the R2 type following the specifications of International Commission on Illumination [11]. R2 road type has a specular factor S1 of 0.582 and an average luminance coefficient Q_0 of 0.07, which result in mixed diffuse and specular reflections [5]. For the vehicle, we assume gloss black paint as in [4]. The wavelength dependent reflectance of glossy black paint and the asphalt road surface are defined in [12] and [13], respectively.

In Fig. 2, we present both the proposed PL model in (4) and the widely used Lambertian model in (1) for the three TLs under investigation. The PL plots are obtained using ray tracing with the measured radiation pattern also included. It is observed that the proposed PL expression in (4) offers a good match with the simulation results for the three TLs. It is also observed that the PLs are significantly different from those based on Lambertian model. For example, for Audi A5 ($i = b$) and for $d = 25$ m, the measured PL is -67 dB, which is lower by ~3 dB and ~4 dB compared with Lambertian model with $\theta_{1/2}$ of 47° and 55°, respectively, see Fig. 2. Note that only Nissan TL ($i = c$) offers higher losses than the Lambertian model. This is due to Lambertian model, see (1), based on HPAs $\theta_{1/2}$, which are 22° and 27° for the left and right TLs in Nissan, respectively. However, these angles do not consider the orientation of the light profile that might be shifted with respect to the 0°
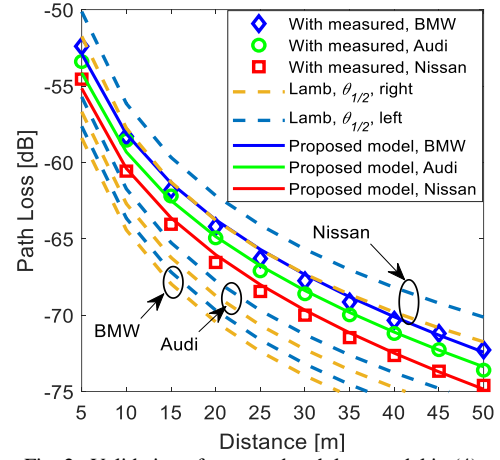

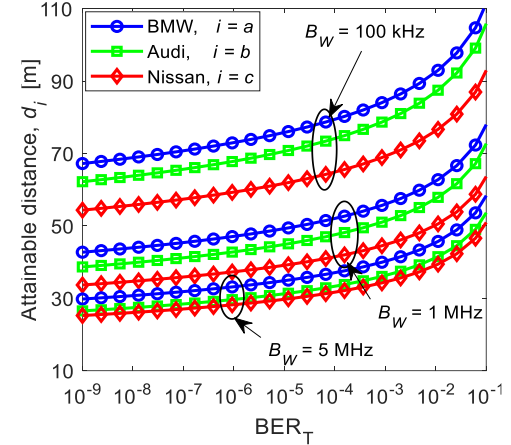Fig. 2. Validation of proposed path loss model in (4).

Fig. 3. Attainable distance vs. the BER for all TLs under investigation.

direction, which is the case in Nissan TL. By considering the real pattern of the light source, which is obtained by empirical measurements, a more realistic path loss can be determined. It is shown in Fig. 2 that, unlike BMW and Audi A5, the path loss based on the measured pattern for Nissan TL is higher than Lambertian by an average of 3 dB.

In Fig. 3, we show the attainable transmission distance d_i as a function of the target BER for three TLs. It is observed that, reducing B_w has a significant impact on d. This is because reducing B_w decreases the noise variance thus resulting in an increase in the received SNR. Therefore, d becomes larger, see Fig. 3. For example, for $B_w = 1$ MHz and a target BER (BER$_T$) of 10^{-3}, which is within the forward error correction BER limit, d_i values are ~55, ~51, and ~44.5 m for BMW, Audi, and Nissan, respectively. These increases to 80, 75, and ~66 m, respectively for B_w 100 kHz.

To investigate the effect of reflections from neighboring vehicles, we consider a V2V system with the TLs of the front vehicle (i.e., BMW with $i = a$) and a single PD located in the front of the vehicle in behind are used as the transmitters and receiver, respectively. We consider three different scenarios and determine their root-mean-square (RMS) delay spreads (τ_{RMS}). The V2V scenarios under consideration are described as:

Scenario 1: Two vehicles are travelling in a single-lane road and are separated by d. This scenario is considered as the best case since there are no neighboring vehicles as in Fig. 4(a).

Scenario 2: A two-lane road with single-side neighboring

vehicle is considered. The two communicating vehicles are separated from each other by d. On the other side, the vehicle traveling at center of the adjacent lane is positioned at an equal distance between the two communicating vehicles, i.e., $d/2$, see Fig. 4(b). **Scenario 3:** A three-lane road with vehicles in all three lanes is considered, see Fig. 4(c).

Fig. 5 illustrates the RMS delay spread as a function of d for the three scenarios. It is observed in Scenario 1 that, there are increased levels of road reflections at shorter distances (i.e., $d \leq$ 15 m) compared to longer distances. At $d \geq 15$ m, the delay spread becomes almost constant and negligible (i.e., NLoS paths becoming less important than the LOS path). In scenarios 2 and 3, the RMS delay spread becomes significant because of additional reflection-induced multipath components from the neighboring vehicles. For example, at d of 25 m, the RMS delay spread for scenarios 1, 2, and 3 are 6×10^{-3}, 0.15, and 0.2 ns, respectively.

Notice that, the RMS delay spread depends on the geometry of the V2V system (i.e., location of the neighboring vehicles). When a reflecting object is located at a distance where the reflected rays have smaller angle of arrivals within the AFOV of the Rx, significant power can be received from the NLoS components, which reach the Rx at different times with respect to the LoS path. Hence, leading to higher delay spread values. The reflected rays with larger arrival angles than the AFOV of the Rx , however, will not be captured by the Rx and hence do not affect either the path loss or the delay spread. Because of this, the delay spread might increase at some distances (i.e., $d =$ 20 and 25 m), slightly reduces at others (i.e., $d =$ 40 and 50 m), or sharply reduces at $d =$ 10 and 15 m. This means that, when larger numbers of neighboring vehicles are considered, depending on the traffic scenario, the effect of the delay spread might be more and therefore should be considered in the design of V2V systems.

VI. CONCLUSION

We investigated the impact of optical radiation pattern of TLs obtained from empirical measurements on the optical PL of vehicular VLC channel. Measurements revealed that the radiation pattern of TLs is not symmetrical, which depends on the TL type, and has a significant impact on the PL compared with Lambertian model. Therefore, a new path loss model was proposed, which provides an excellent match with simulation results obtained by the agreed approach of reference channel models of IEEE 802.15.13 and 802.11bb standards. This model can be practically applied for TLs of different brands and then can be easily adopted to estimate the network performance of V2V systems. Based on this model, we derived the attainable transmission distance for reliable communications. By allowing a communication with 100 kHz bandwidth and up to 66 m distance, VLC based V2V can be positioned as a potential to be used for most of vehicular safety applications utilizing the TL of the vehicle as wireless transmitter and illumination source.
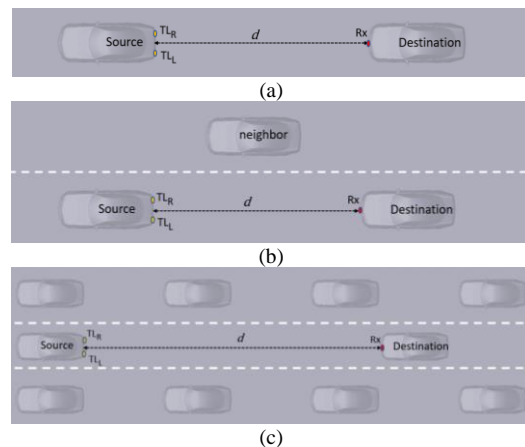
(a)

(b)

(c)

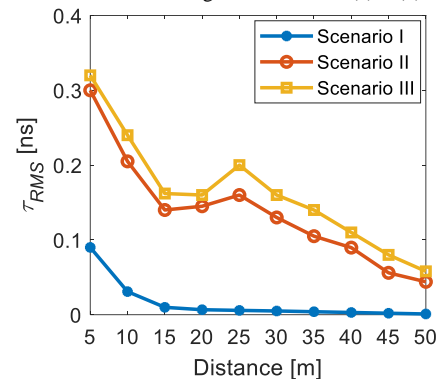Fig. 4. V2V scenarios assuming BMW vehicle: (a) I, (b) II, and (c) III.

Fig. 5. The delay spread vs. the transmission distance for three V2V scenarios.

REFERENCES

[1] Z. Ghassemlooy *et al*., "Emerging optical wireless communications -advances and challenges", *IEEE JSAC*, vol. 33, no. 9, pp. 1738–1749, 2015.

[2] M. Z. Chowdhury *et al*., "A Comparative survey of optical wireless technologies: architectures and applications," *IEEE Access*, vol. 6, pp. 9819-9840, 2018.

[3] A. Al-Kinani *et al*., "Optical wireless communication channel measurements and models", *IEEE Comm. Surv. & Tut*., vol. 20, no. 3, pp. 1939–1962, 2018.

[4] M. Karbalayghareh *et al*., "Channel modelling and performance limits of vehicular visible light communication systems", *IEEE Trans. Veh. Technol.*, vol. 69, no. 7, pp. 6891-6901, July 2020.

[5] P. Luo *et al*., "Performance analysis of a car-to-car visible light communication system", *Appl. Opt.*, vol.54, no.7, pp. 1696–1706, 2015.

[6] A. Memedi, H.-M. Tsai, and F. Dressler, "Impact of realistic light radiation pattern on vehicular visible light communication," *IEEE Global Telecommun. Conf. (GLOBECOM)*, Singapore, pp. 1–6, 2017.

[7] W. Viriyasitavat *et al*., "Short paper: Channel model for visible light communications using off-the-shelf scooter taillight," *2013 IEEE Veh. Netw. Conf. (VNC)*, IEEE, 2013, pp. 170–173.

[8] H.-Y. Tseng *et al*., "Characterizing link asymmetry in vehicle-to-vehicle visible light communications," *2015 IEEE Veh. Netw. Conf. (VNC)*, IEEE, pp. 88–95, 2015.

[9] H. B. Eldeeb *et al*., "Vehicular visible light communications: The impact of taillight radiation pattern," *IEEE Photon. Conf., IPC* 2020.

[10] H. B. Eldeeb *et al*., "Channel modelling for light communications: validation of ray tracing by measurements," *12th Int. Symp. Commun. Sys. Netw. & Digit. Signal Process. (CSNDSP)*, IEEE/IET 2020.

[11] CIE, Calculation and measurement of luminance and illuminance in road lighting: computer program for luminance, illuminance, and glare (Bureau Central de la CIE, 1976).

[12] ASTER Spectral Library-Version 2.0, http://speclib.jpl.nasa.gov.

[13] Adrian *et al*., "*Influence of pavement reflectance on lighting for parking lots*", Skokie, IL: Portland Cement Association, 2005.